Making the Medicines of Tomorrow

ENTROPIC BIOSCIENCES | Lonza

A scalable primary-cell-based 3D human skin organoid platform

For barrier biology and injury response studies

Reihaneh Haghniaz[1], Ethan Borokhovich[1], Koh Meng Aw Yong[2], Emma Hoffman[3], Anshika Sharma[3], Amir Nasajpour[1]

1. Entropic Bioscience, Inc. USA; 2. Lonza Walkersville, USA; 3. Lonza Durham, USA

Human skin models that combine physiological relevance with high throughput screening capability remain limited. In this study, we describe a 96-well compatible self-organizing 3D human skin organoid platform generated by co-seeding primary adult normal human epidermal keratinocytes (NHEK) and adult normal human dermal fibroblasts (NHDF) in ZYRALIX™ coated plates using a mixed-medium workflow. Co-seeded cells assembled into compact organoids that developed bilayer epidermal-dermal organization within the first 66 hours that continued to mature over 21 days. The resulting organoids demonstrated structural maturation, functional barrier formation, long-term viability, and dose-dependent responses to ultraviolet (UV) injury. These findings support the use of this primary cell-based 3D skin organoid as a scalable, *in vitro* platform for studying barrier biology, dermatotoxicology, and environmental insult testing.

Introduction

There is a growing need for *in vitro* skin models that provide greater physiological relevance than conventional two-dimensional culture while remaining practical for scalable experimentation. Traditional monolayer systems are useful for cell assays but lack the multicellular organization, extracellular matrix interactions, and tissue-like architecture required to model functions such as epidermal differentiation, barrier formation, and coordinated injury responses[1].

Three-dimensional culture systems offer an opportunity to address these limitations by enabling primary cells to organize into more tissue-relevant structures[1]. However, many advanced skin models require complex workflows, extended maturation timelines, specialized handling, or lower-throughput formats that can limit their use in screening oriented applications[2].

Skin is especially well suited for scalable 3D modeling because of its role as a barrier tissue and its frequent exposure to environmental, chemical, and physical stressors[3]. A practical model that captures key features of epidermal-dermal organization, barrier-associated function, and injury responsiveness in a plate-based format could support both mechanistic studies and earlier stage screening workflows.

Here, we describe a primary cell-based 3D human skin organoid system generated by co-seeding normal human epidermal keratinocytes and normal human dermal fibroblasts directly into ZYRALIX™ Platform coated 96-well plates. The resulting organoids self-organize into bilayer structures, mature over time, exhibit barrier-associated properties, and respond to ultraviolet injury, supporting their potential use as a scalable *in vitro* platform for skin biology and dermatotoxicology applications.

Material and Methods

Cell source and culture media

Lonza's cryopreserved normal human dermal fibroblasts (NHDF-Ad; Lonza, CC-2511) and cryopreserved adult normal human epidermal keratinocytes (NHEK-Ad; Lonza, 00192627) were used to generate 3D human skin organoids. NHDF were cultured in Fibroblast Basal Medium (FBM®; Lonza, CC-3131) supplemented with FGM® 2 SingleQuots® (Lonza, CC-4126), while NHEK cells were cultured in Keratinocyte Basal Medium Gold (KBM® Gold; Lonza, 00192151) supplemented with KGM® Gold SingleQuots® (Lonza, 00192152).

FBM® Basal Medium supplemented with FGM® 2 SingleQuots®, whereas NHEK were cultured in KBM® Gold Basal Medium supplemented with KGM® Gold SingleQuots®.

Complete FGM® Culture Media was prepared by adding Lonza FBM® Basal Medium (Cat. no. CC-3131) and FGM® 2 SingleQuots® (Cat. no. CC-4126). Components were first thawed and brought to room temperature before mixing. Complete KGM® Medium was prepared by adding Lonza KBM® Gold Basal Medium (00192151) with KGM® Gold SingleQuots® (Cat. no. 00192152). Components were first thawed and brought to room temperature before mixing. Media was stored at 4°C when not in use.

Cell recovery and expansion

Each cell type was thawed and expanded separately under standard culture conditions at 37°C and 5% CO_2. Culture media were refreshed every other day until cells reached approximately 80 to 90% confluency until approximately 80 to 90% confluency. For NHEK, growth medium was changed 24 hours post-thaw to remove residual cryoprotectant and non-adherent cells, followed by subsequent media changes every other day. NHDF cells were expanded using the same general workflow, and both cell types were harvested before over-confluence to preserve performance characteristics.

Cell harvest and counting

Confluent cells were rinsed with Dulbecco's phosphate-buffered saline (DPBS; Gibco) and dissociated using TrypLE™ Express (Gibco). Enzymatic dissociation was neutralized using Trypsin Neutralizing Solution (Lonza, CC-5002), harvested and collected by centrifugation at 1200 rpm for 5 minutes. Cell pellets were resuspended in their respective complete growth media and quantified using a digital cell counter (Countless 3 FL, Invitrogen). Viability percentages were recorded for each cell population prior to co-seeding.

Organoid assembly in 96-well format

For organoid generation, NHEK and NHDF were combined at a 1:1 ratio at total seeding densities of 25,000, 50,000, or 100,000 cells per well (e.g., 50,000 NHEK and 50,000 NHDF for a total of 100,000 cells). Cells were suspended in 200 µL of mixed culture medium prepared by combining keratinocyte and fibroblast complete media at a 1:1 ratio.

The cell suspension was dispensed into ZYRALIX™ Platform coated 96-well plates and incubated at 37°C and 5% CO_2. Plates were left undisturbed for 24 hours to facilitate cell aggregation and early tissue organization. Media changes were performed every other day using gentle pipetting to avoid disruption of the developing organoids. Organoids were maintained in culture for up to 21 days.

Morphological and structural characterization

Organoid formation and size evolution were assessed by brightfield imaging over a 21-day culture period. Early cell distribution and bilayer organization were evaluated using

CellTracker™ Fluorescence imaging at 0, 24, and 66 hours following co-seeding. Keyence BZ-X Series fluorescence microscope with z-stack image acquisition was used to capture the 3D organization of the developing organoids. Prior to organoid formation, NHDF cells were labeled with CellTracker™ Red CMTPX dye (Invitrogen, Cat# C34552), while NHEK cells were labeled with CellTracker™ Green CMFDA dye (MedChemExpress, Cat# HY-126561) at a final concentration of 5 µM in their respective culture media and incubated for 8 hours before co-seeding.

Structural maturation was examined by immunofluorescence staining for vimentin, cytokeratin-14 (CK14), collagen IV, laminin-5, and loricrin, and by hematoxylin and eosin (H&E) histology at specified maturation time points.

Barrier function and viability assay

Barrier function was assessed by monitoring the diffusion of fluorescent dye into organoids over time using CellTracker™ Red CMTPX dye (Invitrogen, Cat. no. C34552). Organoids were exposed to the fluorescent tracer at a final concentration of 5 µM and imaged every 15 minutes for up to 7 hours using the IncuCyte® S3 Live-Cell Analysis System (Essen BioScience). Keratinocyte-containing bilayer organoids were compared with fibroblast-only organoids to evaluate the contribution of the epidermal compartment to permeability control. Long-term viability was analyzed LIVE/DEAD™ Viability/Cytotoxicity Kit, for mammalian cells (Invitrogen, Cat. no. L3224) and by lactate dehydrogenase assay kit (LDH, abcam, Cat. no. ab102526) at days 7, 14, and 21.

QPCR Methods

Skin organoid spheroids were cultured for 14 days under five commercially available scaffold or surface conditions including ZYRALIX™ Platform coated wells. Relative gene expression was determined using the comparative ΔCt method, where ΔCt = Ct Target – Ct Housekeeping, and the resulting ΔCt values were used for comparison between the different organoid culture conditions. Housekeeping gene GADPH primer sequence Fw: GTCTCCTCTGACTTCAACAGCG Rv: ACCACCCTGTTGCTGTAGCCAA; CK14 Basal layer/Differentiation marker Fw: TGCCGAGGAATGGTTCTTCACC Rv: GCAGCTCAATCTCCAGGTTCTG.

UV injury model

To evaluate environmental insult responsiveness, organoids were allowed to form and mature for 5 days before exposing to UV radiation at 6 or 9 kJ/cm² and allowed to recover for 24 hours. On day 6, organoids were analyzed using live/dead imaging, tested for barrier permeability, histology, and cytokine measurements for IL-6 and IL-1α (Abcam, ab178013 and ab178008) in culture supernatants.

Results

Self-assembly of bilayer skin organoids within 24 hours

Following co-seeding of NHDF and NHEK into ZYRALIX™-coated wells, cells rapidly assembled into compact 3D organoids. Based on time course fluorescence imaging, both NHDF and NHEK cell populations were broadly dispersed at the time of seeding; by 24 hours, keratinocytes had begun to localize to a continuous outer layer while fibroblasts concentrated centrally; and by 66 hours, the co-culture displayed a distinct bilayer arrangement. These observations suggest that the system supports rapid tissue self-organization soon after plating (Fig. 1).

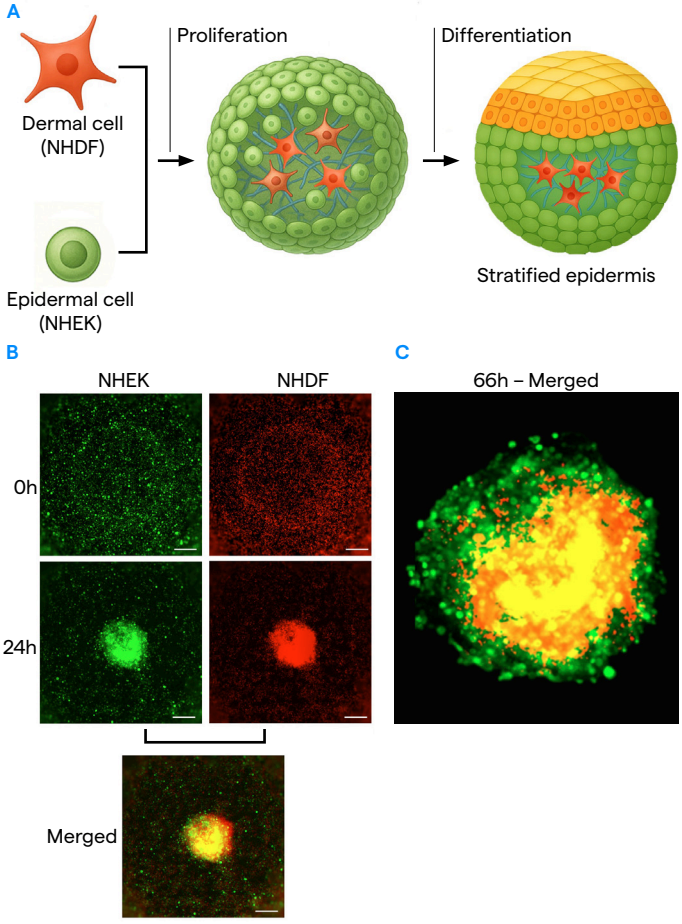

Figure 1. Rapid 3D bilayer assembly of NHEK-NHDF skin organoids. (A) Schematic showing co-aggregation and spatial organization of normal human epidermal keratinocytes (NHEK; green) and normal human dermal fibroblasts (NHDF; red) into 3D bilayer skin organoids on ZYRALIX™-coated surfaces. Over 66 hours, NHEK localized toward the organoid periphery, forming an epidermis-like outer layer, while NHDF localized toward the center, forming a dermal-like core. (B) Time-lapse fluorescence images of CellTracker™ labeled NHEK and NHDF at 0, 24, and 66 hours post-seeding, showing progressive cell type-specific organization. (C) Enlarged merged CellTracker™ image at 66 hours highlighting the epidermis-like outer compartment surrounding a fibroblast-rich core. Scale bar: 500 µm.

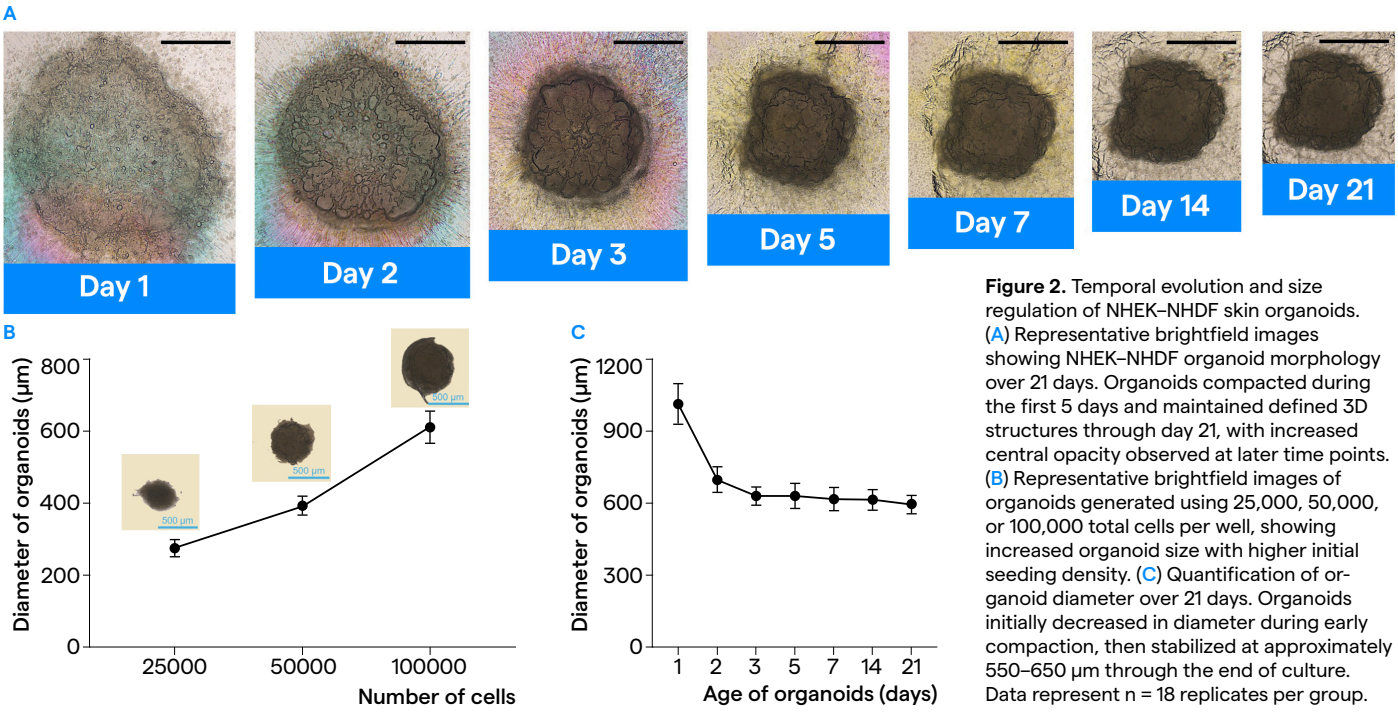

Figure 2. Temporal evolution and size regulation of NHEK–NHDF skin organoids. (A) Representative brightfield images showing NHEK–NHDF organoid morphology over 21 days. Organoids compacted during the first 5 days and maintained defined 3D structures through day 21, with increased central opacity observed at later time points. (B) Representative brightfield images of organoids generated using 25,000, 50,000, or 100,000 total cells per well, showing increased organoid size with higher initial seeding density. (C) Quantification of organoid diameter over 21 days. Organoids initially decreased in diameter during early compaction, then stabilized at approximately 550–650 µm through the end of culture. Data represent n = 18 replicates per group.

Controlled size evolution and compatibility with high-throughput culture

Brightfield imaging over 21 days showed that organoids compacted during the first several days post seeding before reaching a relatively stable diameter. Measurements indicate that organoids settled into a size range of approximately 550 to 650 µm after an initial decrease during early culture. In addition, increasing the starting cell number from 25,000 to 100,000 total cells per well produced proportionally larger organoids, demonstrating a tunable relationship between seeding density and final organoid size. Together, these observations support a controllable and reproducible formation of different sized skin organoids in a high-throughput 96-well format (Fig. 2).

Progressive structural maturation and epidermal differentiation

Immunostaining across days 7, 14, and 21 demonstrated progressive maturation of the organoids. Vimentin-positive fibroblasts populated an inner dermal-like compartment, whereas cytokeratin-14-positive basal keratinocytes formed an external epithelial compartment. Additional staining revealed collagen IV and laminin-5 deposition at the dermal-epidermal interface, consistent with basement membrane-associated matrix organization[4,5]. Loricrin expression was observed in the upper epidermal layers, consistent with terminal differentiation[6]. H&E staining further demonstrated a multilayered outer shell surrounding a fibroblast-rich core. These suggest that the organoids develop beyond simple aggregation and display key structural hallmarks of differentiated skin tissue

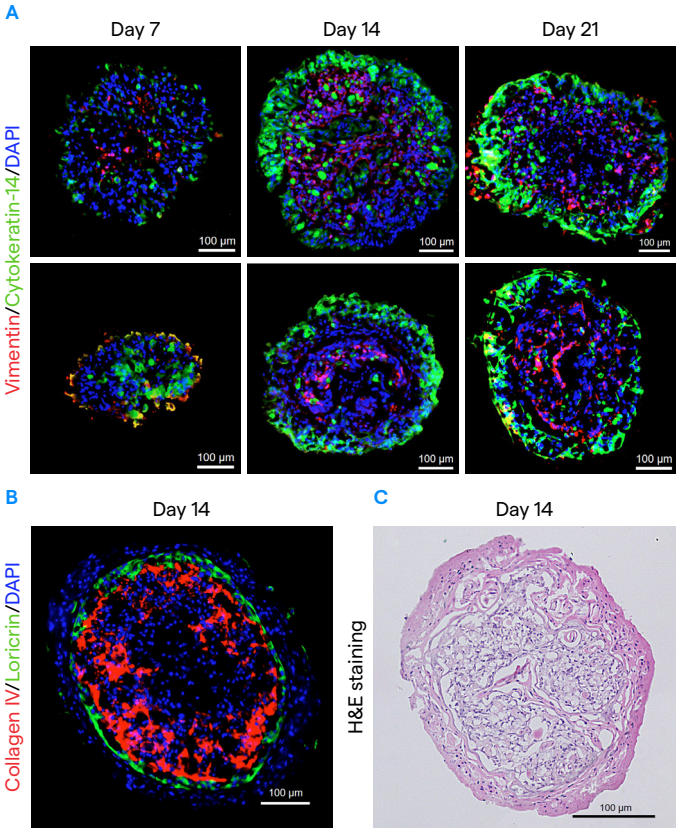

Figure 3. Structural maturation and epidermal differentiation of ZYRALIX™ generated 3D bilayer human skin organoids. (A) Immunofluorescence imaging of ZYRALIX™ skin organoids at days 7, 14, and 21 stained for vimentin (red), cytokeratin-14 (CK14; green), and DAPI (blue). Over time, vimentin positive fibroblasts localized within the inner compartment, while CK14 positive keratinocytes formed an outer epithelial-like layer. (B) Higher-resolution immunostaining of a day 14 organoid showing collagen IV (red) near the dermal-epidermal-like interface and loricrin (green) within the outer epidermal-like compartment, indicating matrix deposition and terminal keratinocyte differentiation. (C) H&E staining of a day 14 organoid showing a multilayered outer epithelial-like region surrounding a fibroblast-rich core. Scale bars: 100 µm.

(Fig. 3). Furthermore, ZYRALIX™ Organoids exhibit robust cytokeratin-14 (CK-14) expression comparable to native skin tissue, when compared to several conventional organoid culture systems, supporting effective basal keratinocyte phenotype maintenance and epidermal-like compartment formation (Fig. 4).

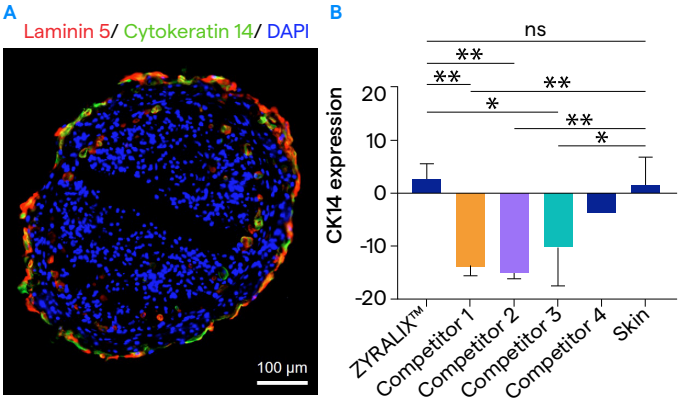

Figure 4. Basement membrane-associated matrix deposition and epidermal marker expression in ZYRALIX™ derived 3D skin organoids. (A) Representative immunofluorescence image of a day 14 ZYRALIX™ skin organoid stained for cytokeratin-14 (CK14; green), laminin-5 (red), and DAPI (blue) nuclear counterstain. CK14 identifies basal keratinocytes within the epidermal-like compartment, while laminin-5 staining is observed near the dermal–epidermal-like interface, supporting basement membrane-associated matrix organization within the organoid. Scale bar: 200 µm. (B) Quantitative comparison of normalized CK14 gene expression at day 14 across ZYRALIX™ organoids and commercially available low-attachment culture platforms, with *ex vivo* adult skin included as a physiological reference. Error bars represent standard deviation.

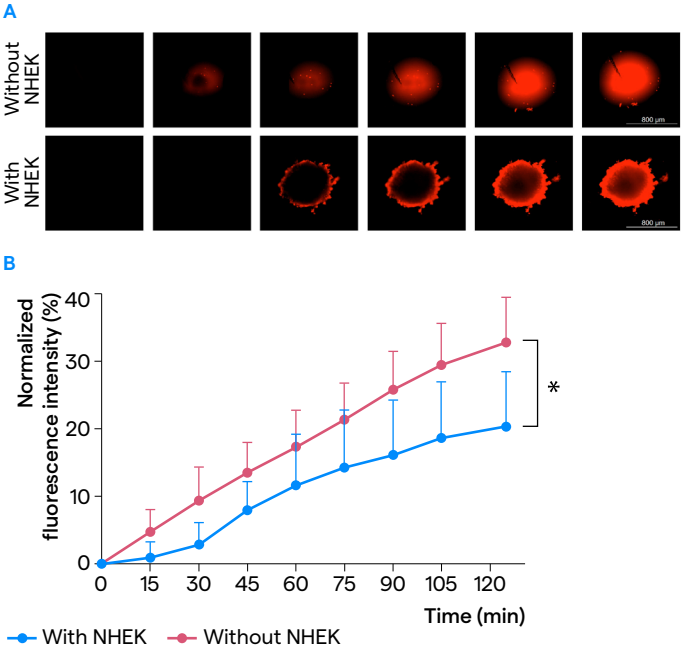

Figure 5. Keratinocyte incorporation reduces dye permeability in ZYRALIX™ 3D skin organoids. (A) Time-lapse fluorescence imaging of dye diffusion into fibroblast-only and fibroblast-keratinocyte bilayer organoids at 0, 30, 60, 120, 180, and 240 minutes following dye exposure. Fibroblast-only organoids showed greater fluorescence accumulation over time, whereas NHEK-containing bilayer organoids showed reduced dye penetration. (B) Quantification of normalized fluorescence intensity over time, showing higher permeability in fibroblast-only organoids compared with NHEK-containing bilayer organoids. Data are presented as mean ± SD; statistical significance is indicated by $p < 0.05$.

Keratinocyte incorporation supports barrier function

Functional analysis of permeability demonstrated that organoids containing keratinocytes exhibited substantially reduced dye penetration over time relative to fibroblast-only organoids. Quantified fluorescence intensity curves showed lower permeability in the bilayer organoids, indicating that the inclusion of NHEK cells contributed to the formation of an epidermal barrier that limits molecular diffusion (Fig. 5).

Long-term viability and culture stability

Live/dead imaging and LDH-based viability analysis demonstrated that the organoids maintained high viability through 21 days of culture. Viability of organoids formed on the ZYRALIX™ Platform across days 7, 14, and 21 ranged between approximately 85 to 95%. The organoids also display structural stability at later time points, supporting the suitability of the platform for studying long-term skin biology and for use in longitudinal studies (Fig. 6).

Dose-dependent response to UV-induced environmental injury

To test responsiveness to environmental insult, organoids were exposed to UV radiation on day 5 and analyzed one day post recovery. UV treatment reduced tissue viability in a dose-dependent manner, with more pronounced loss of viable tissue at 9 kJ/cm² than at 6 kJ/cm² (Fig 8.). UV exposure also increased dye penetration, indicating barrier disruption, and histological sections showed progressive structural damage with increasing UV doses. In parallel, culture supernatants displayed elevated levels of IL-6 and IL-1α following irradiation[7,8], demonstrating activation of inflammatory signaling pathways in response to injury (Fig. 9). These results indicate that the organoids develop tissue-like organization and retain functional responsiveness to external stressors.

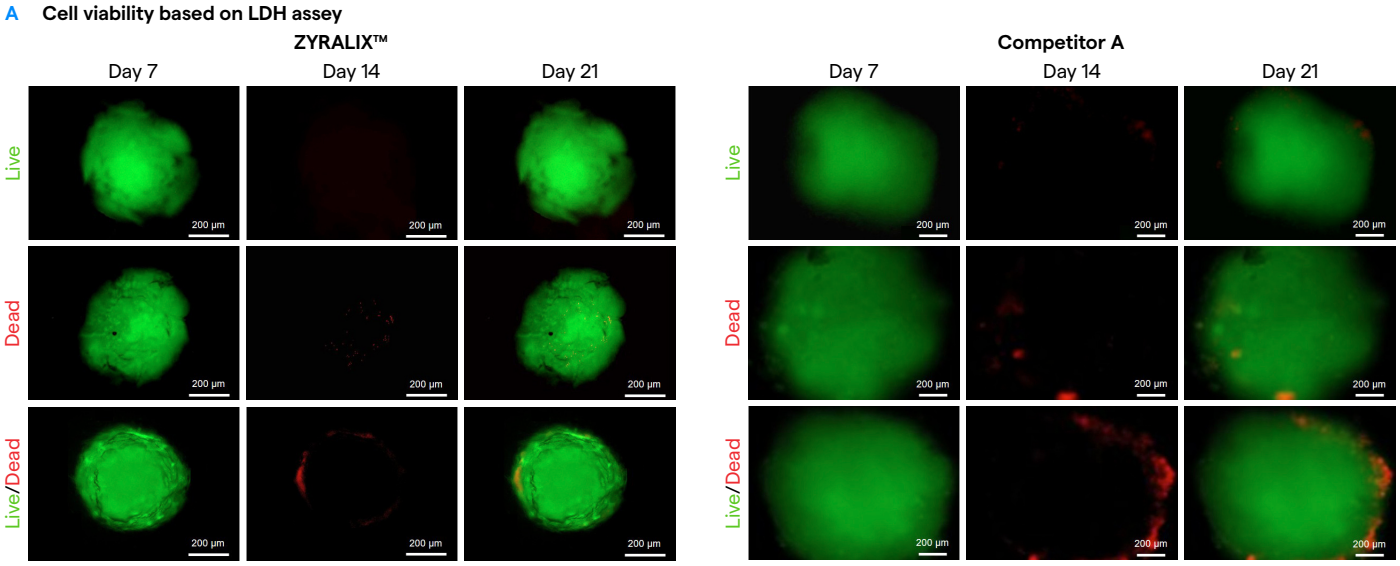

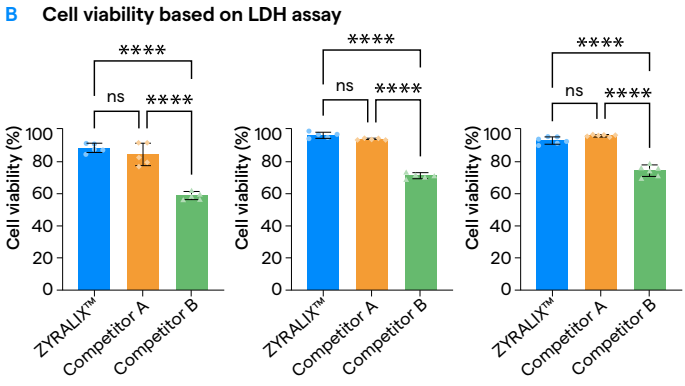

Figure 6. Long-term viability of 3D skin organoids cultured on ZYRALIX™ Platform and commercial low-attachment platforms. (A) Live/Dead staining at days 7, 14, and 21 showed that ZYRALIX™ organoids maintained viability and structural integrity through day 21, while ULA-VB organoids exhibited increased cell death and reduced morphology over time. Scale bars: 200 µm. (B) LDH-based viability analysis demonstrated that ZYRALIX™ organoids maintained high viability (approximately 85–95%) over 21 days, with significantly greater viability than NTC-UB organoids and comparable performance to ULA-VB. Data are presented as mean ± SD; one-way ANOVA. ns = not significant; *p < 0.05; **p < 0.01; ***p < 0.001; ****p < 0.0001; n ≥ 5 replicates per group.

Scheme

Experimental workflow for UV radiation evaluation using ZYRALIX™ 3D human skin organoids

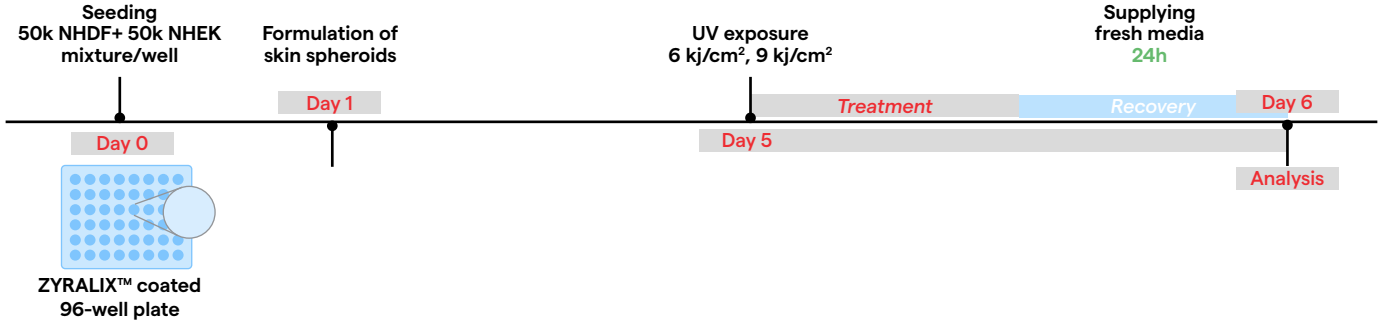

Figure 7. Experimental workflow for UV injury assessment using ZYRALIX™ Platform 3D human skin organoids. Normal human dermal fibroblasts (NHDF) and normal human epidermal keratinocytes (NHEK) were co-seeded at a 1:1 ratio, with 50,000 cells of each type per well, into ZYRALIX™ coated 96-well plates on day 0. Organoids self-assembled within 24 hours and were cultured through day 5 prior to ultraviolet (UV) exposure. On day 5, organoids were exposed to defined UV doses of 6 or 9 kJ/cm², followed by media replacement and a 24-hour recovery period. On day 6, organoids and culture supernatants were analyzed using multiparametric readouts to assess viability, barrier permeability, tissue morphology, and inflammatory cytokine release.

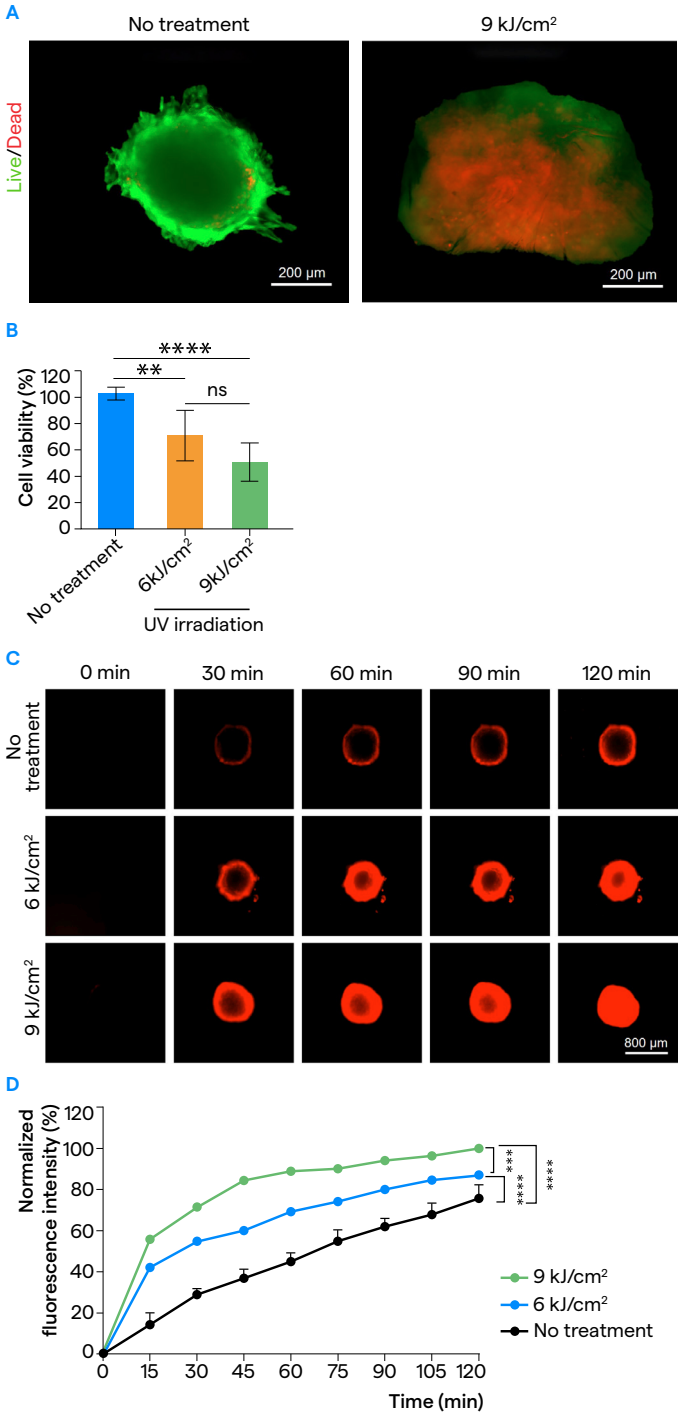

Figure 8. UV-induced cytotoxicity and barrier disruption in ZYRALIX™ 3D bilayer human skin organoids. (A) Representative Live/Dead fluorescence images of ZYRALIX™ skin organoids following UV exposure. Untreated organoids showed predominantly viable cells, while organoids exposed to 9 kJ/cm² UV displayed increased dead-cell staining and reduced viable tissue. Scale bar: 200 µm. (B) Quantification of organoid viability following UV exposure. Treatment with 6 or 9 kJ/cm² UV reduced viability compared with untreated controls, consistent with dose-associated UV cytotoxicity. Data are presented as mean ± SD; statistical significance is indicated as ns = not significant; **p < 0.01; ****p < 0.0001. (C) Time-lapse fluorescence imaging of dye diffusion into organoids following UV exposure. Untreated organoids showed limited dye penetration, whereas UV-treated organoids displayed increased fluorescence accumulation over time, indicating increased permeability. Images were acquired at 0, 30, 60, 90, and 120 minutes following dye exposure. Scale bar: 500 µm. (D) Quantification of normalized fluorescence intensity over time. UV-treated organoids showed increased fluorescence intensity compared with untreated controls, with the 9 kJ/cm² condition producing the greatest permeability increase. Together, these results demonstrate dose-associated effects of UV exposure on organoid viability and barrier-associated permeability.

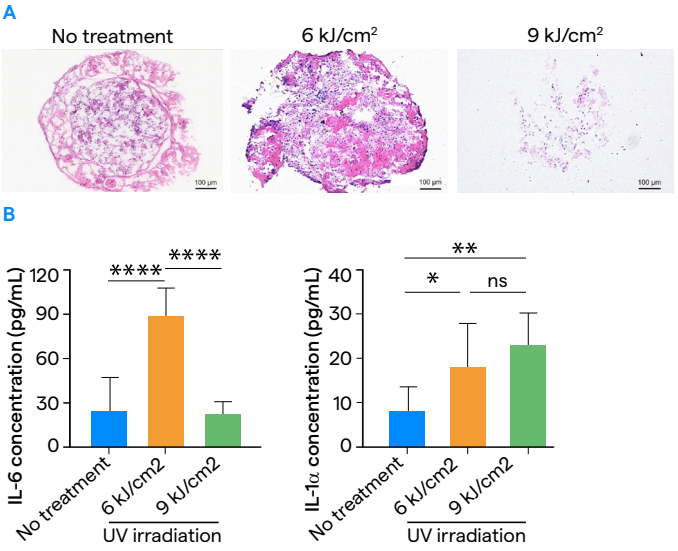

Figure 9. UV-induced tissue damage and inflammatory cytokine release in ZYRALIX™ 3D bilayer human skin organoids. (A) Representative H&E-stained sections of ZYRALIX™ skin organoids following UV exposure. Untreated organoids maintained organized tissue-like architecture, whereas exposure to 6 kJ/cm² UV resulted in partial structural disruption and cellular damage. Exposure to 9 kJ/cm² UV produced more pronounced tissue disruption and loss of structural integrity. Scale bar: 100 µm. (B) Quantification of inflammatory cytokines in culture supernatants following UV exposure. IL-6 and IL-1α levels were measured by immunoassay. UV exposure increased cytokine release relative to untreated controls, with the 6 kJ/cm² condition producing the highest IL-6 response and IL-1α increasing in a dose-associated manner. Data are presented as mean ± SD. Statistical significance is indicated as ns = not significant; *p < 0.05; **p < 0.01; ***p < 0.001.

Discussion

This study describes a scalable 3D human skin organoid model that combines primary human cell biology, self-organization, and compatibility with 96-well plate-based workflows. By co-seeding normal human epidermal keratinocytes and normal human dermal fibroblasts in ZYRALIX™ Platform coated plates, organoids formed reproducibly and developed epidermal-dermal-like compartmentalization within the first 66 hours of culture.

The resulting structures displayed features not typically captured in conventional monolayer systems, including multicellular organization, epidermal marker expression, basement membrane-associated matrix deposition, barrier-associated reduction in dye permeability, and sustained viability over 21 days. Importantly, the organoids also demonstrated functional responsiveness to ultraviolet injury, as shown by dose-associated changes in viability, permeability, tissue structure, and inflammatory cytokine release.

The model is not intended to fully replicate the complexity of native human skin or more advanced reconstructed skin systems. Rather, it provides a practical platform between simple 2D culture and complex tissue models, with potential utility for applications where tissue-like organization, primary human biology, and experimental scalability are important.

Future development may include incorporation of additional skin-relevant cell types, such as immune, endothelial, or vascular-associated populations, as well as expanded benchmarking against established skin models and compound response datasets. These enhancements could further extend the platform's relevance for dermatotoxicology, barrier biology, inflammation research, and environmental insult testing.

Conclusion

This report describes a high-throughput 3D human skin organoid platform generated by co-seeding primary NHEK and NHDF in ZYRALIX™ Platform coated 96-well plates. The workflow uses readily available cryopreserved primary cells and standard media, producing rapid self-assembly into bilayer organoids, promoting maturation through day 21, and enabling multiparametric characterization of skin biology including morphology, structure, barrier function, viability, and inflammatory injury responses. The resulting model provides a scalable and controllable system for dermatotoxicology, barrier biology, and environmental insult studies.

Entropic Acknowledgements
This project has been funded in whole or in part with Federal funds from the Department of Health and Human Services; Office of the Administration for Strategic Preparedness and Response; Biomedical Advanced Research and Development Authority, under OT number 75A50124C00034.

References:

1. **Kayla Duval, Hannah Grover, Li-Hsin Han, Yongchao Mou, Adrian F. Pegoraro, Jeffery Fredberg, and Zi Chen.** Modeling Physiological Events in 2D vs. 3D Cell Culture Physiology 2017 32:4, 266-277 10.1152/physiol.00036.2016
2. **Teertam S, Setaluri V,** Ayuso J Advances in Microengineered Platforms for Skin Research*, JID Innovations*, 2024; 5
3. **Lim KM.** Skin Epidermis and Barrier Function. Int J Mol Sci. 2021 Mar 16;22(6):3035. doi: 10.3390/ijms22063035. PMID: 33809733; PMCID: PMC8002265.
4. **Alam H, Sehgal L, Kundu ST, Dalal SN, Vaidya MM.** Novel function of keratins 5 and 14 in proliferation and differentiation of stratified epithelial cells. *Mol Biol Cell*. 2011 Nov;22(21):4068-78. doi: 10.1091/mbc.E10-08-0703. Epub 2011 Sep 7. PMID: 21900500; PMCID: PMC3204069.
5. **Pfisterer K, Shaw LE, Symmank D, Weninger W.** The Extracellular Matrix in Skin Inflammation and Infection. *Front Cell Dev Biol*. 2021 Jul 6;9:682414. doi: 10.3389/fcell.2021.682414. PMID: 34295891; PMCID: PMC8290172.
6. **Ishitsuka Y, Roop DR.** Loricrin at the Boundary between Inside and Outside. *Biomolecules*. 2022 May 6;12(5):673. doi: 10.3390/biom12050673. PMID: 35625601; PMCID: PMC9138667.
7. **Nasti TH, Timares L.** Inflammasome activation of IL-1 family mediators in response to cutaneous photodamage. *Photochem Photobiol*. 2012 Sep-Oct;88(5):1111-25. doi: 10.1111/j.1751-1097.2012.01182.x. Epub 2012 Jul 9. PMID: 22631445; PMCID: PMC3435462.
8. **Lee Y, Kim H, Kim S, Shin MH, Kim YK, Kim KH, Chung JH.** Myeloid differentiation factor 88 regulates basal and UV-induced expressions of IL-6 and MMP-1 in human epidermal keratinocytes. *J Invest Dermatol*. 2009 Feb;129(2):460-7. doi: 10.1038/jid.2008.261. Epub 2008 Aug 21. PMID: 18719610.
9. **Lee, T., Kyung, S.Y., Kwon, M.** *et al.* Innovations in skin microphysiological systems for nonclinical testing and FDA modernization. *Microsyst Nanoeng* 12, 44 (2026). https://doi.org/10.1038/s41378-025-01149-1

Contact us

North America
Customer Service: +1 800 638 8174 (toll free)
order.us@lonza.com
Scientific Support: +1 800 521 0390 (toll free)
scientific.support@lonza.com

Europe
Customer Service: +32 87 321 611
order.europe@lonza.com
Scientific Support: +49 221 99199 400
scientific.support.eu@lonza.com

International
Contact your local Lonza distributor
Customer Service: +1 301 898 7025
scientific.support@lonza.com

Lonza Walkersville, Inc. – Walkersville, MD 21793

Learn more.

bioscience.lonza.com